

Supporting Information

Water soluble glucose-appended quinoline-benzothiazole conjugate as a selective and sensitive receptor for Cu⁺ ion in aqueous media and intracellular bio-imaging in live cells

Ravinkumar Valand^a, Nidhi Pandey^b, Jaysh Ballare^b and Areti Sivaiah^{*a}

^a Department of Chemistry, Sardar Vallabhbhai National Institute of Technology, Surat-395007, Gujarat, India. E-mail: aretis@chem.svnit.ac.in

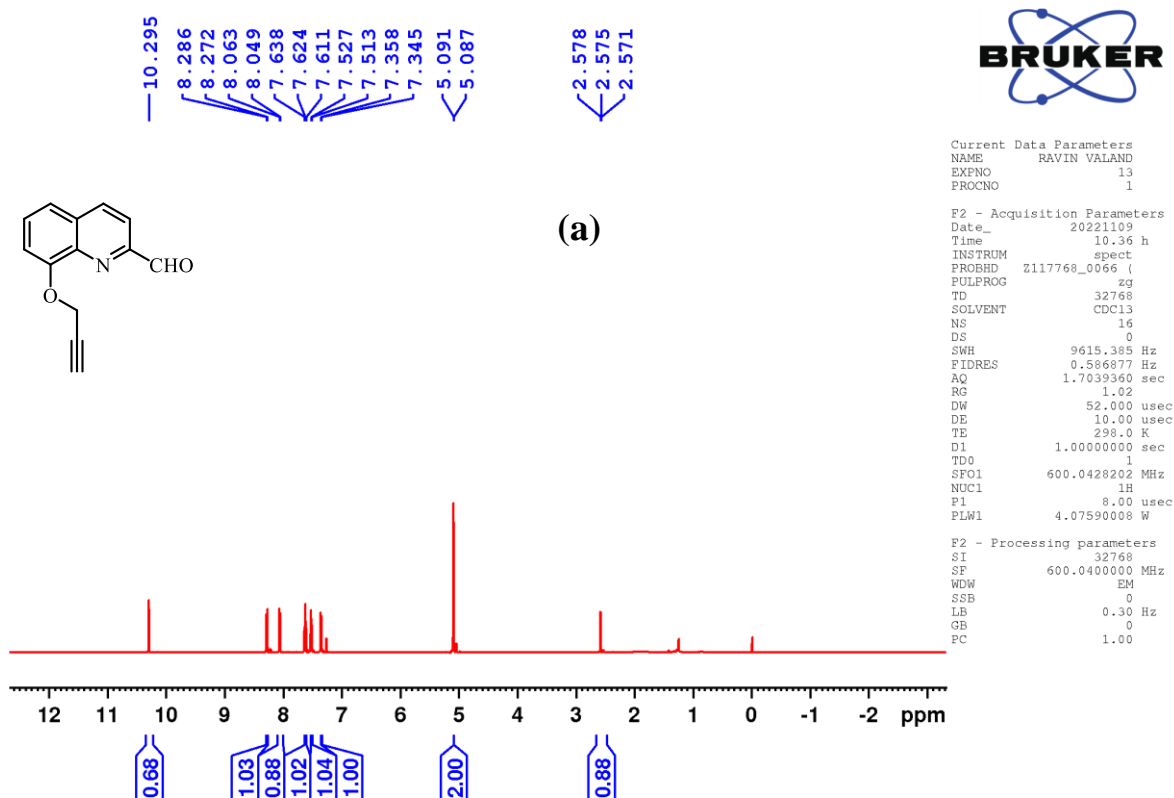
^b Department of Chemical Engineering, Indian Institute of Technology Bombay, Powai-400076, Mumbai, India

Corresponding author: Areti Sivaiah*-Department of Chemistry, Sardar Vallabhbhai National Institute of Technology, Surat-395007, Gujarat, India: Email: aretis@chem.svnit.ac.in

Table of Contents	Page no
S1. Synthesis and characterization of compound P₂	03
S2. Synthesis and characterization of compound P₃	04
S3. Synthesis and characterization of compound P₅	06
S4. Characterization of compound P₆	08
S5. Characterization of compound L	09
S6. Solubility of probe L in water	11
S7. Effect of absorbance and fluorescence on probe L using different metal ions	11
S8. Fluorescence spectra of L with different metal ions	12
S9. Association constant obtained from the fluorescence titration of { L+Cu⁺ } complex	13
S10. Determination of limit of detection (LOD) of Cu⁺ by L	13
S11. Fluorescence quantum yield of L and { L+Cu⁺ } complex	13
S12. Table 1: Comparisons between L and the molecular probe were reported in the literature.	14
S13. Reversibility experiments of L with Cu⁺	16
S14. Optimized structure of L and { L+ Cu⁺ }	17
Table S2. Cartesian coordination of optimized L	17
Table S3. Cartesian coordinates of optimized { L+ Cu⁺ }	18
S15. Effect of pH on the Fluorescence emission of L and { L+ Cu⁺ }	18
References	19

S 01. Synthesis and characterization of compound P₂

The P₂ has been synthesized by a producer in the reported literature¹. In a dry 100 mL round bottom flask, 8-hydroxyquinoline 2-carboxaldehyde (2 g, 11 mmol) and potassium carbonate (2.4 g, 17.3 mmol) were dissolved in *N,N*-dimethylformamide (DMF) and stirred for 5 minutes. Subsequently, a solution of propargyl bromide (1.3 mL, 17.3 mmol) was added dropwise to the reaction mixture. The resulting mixture was stirred at room temperature overnight. Upon completion of the reaction, the mixture was separated using ethyl acetate and water. The organic layer was extracted with ethyl acetate, dried over anhydrous sodium sulfate (Na₂SO₄), and concentrated under a vacuum. The crude product was then purified by column chromatography to yield a brown precipitate (1.94 g, Yield= 80 %) ¹H NMR (CDCl₃, 600 MHz): δ 10.29 (s, 1H), 8.27 (d, *J*=8.46 Hz, 1H), 8.05 (d, *J*=8.45 Hz, 1H), 7.51 (d, *J*=8.15 Hz, 1H), 7.35 (d, *J*=7.74 Hz, 1H), 5.08 (d, *J*=2.31 Hz, 2H), 2.57 (t, *J*=2.30 Hz, 1H) ¹³C NMR (CDCl₃, 150 MHz): δ 193.99, 154.12, 151.96, 140.43, 137.69, 131.73, 129.78, 121.01, 118.28, 111.39, 78.17, 76.95, 57.23



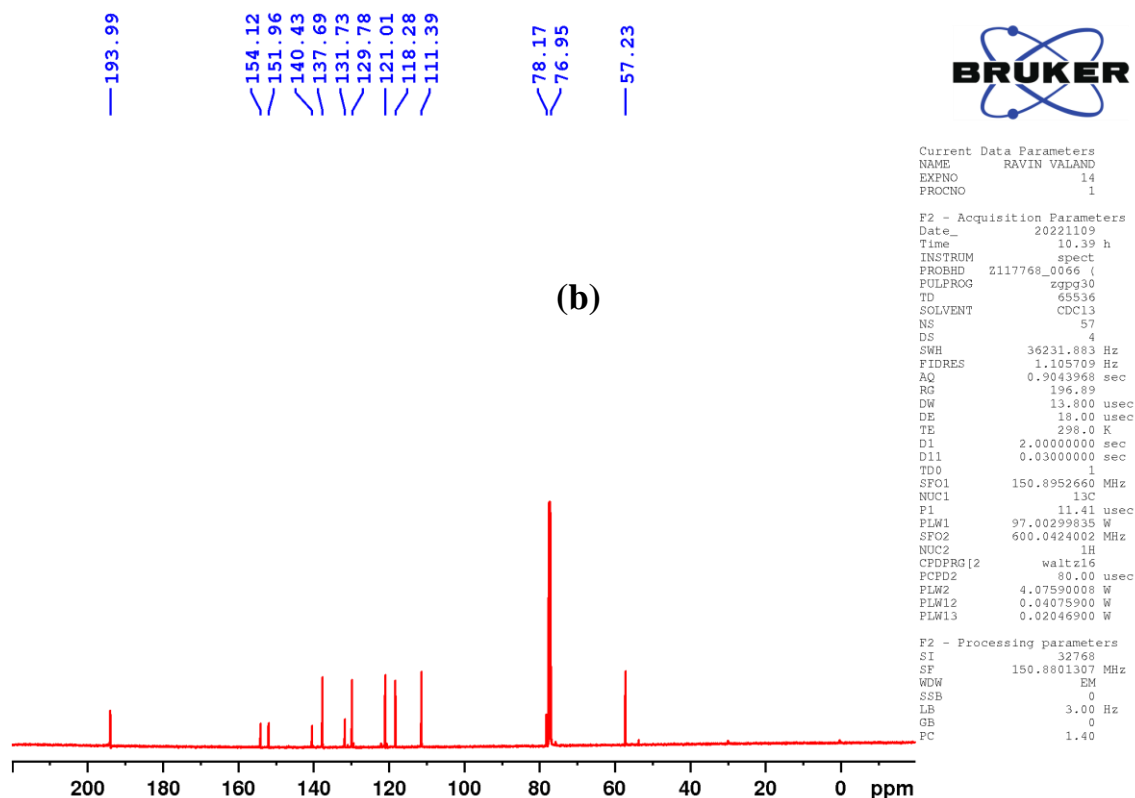


Fig. S1. Spectrum of compound **P₂** in CDCl₃ (a) ¹H NMR (b) ¹³C NMR

S2. Synthesis and characterization of compound **P₃**

P₂ (1 g, 4.7 mmol) and 2-aminobenzene-1-thiol (608 μL, 5.6 mmol) were dissolved in DMSO and stirred at 120 °C for 2 hours. The reaction mixture cooled to room temperature and poured in water. The crude product was extracted with ethyl acetate and washed with water. The Organic layer was dried over anhydrous sodium sulfate and concentrate under vacuum. The crude product was then purified by silica gel column chromatography using a 4:6 mixture of Ethyl acetate and petroleum ether. The pure fraction was collected and evaporated to yield the product (1.12 g, Yield= 75 %) ¹H NMR (CDCl₃, 400 MHz): δ 8.50 (d, *J*=8.57 Hz, 1H), 8.28 (d, *J*= 7.59 Hz, 1H), 8.13 (d, *J*=8.16 Hz, 1H), 7.98 (d, *J*=7.86 Hz, 1H), 7.54-7.50 (m, 1H), 7.45-7.42 (m, 1H), 7.33 (m, 1H) ¹³C NMR (CDCl₃, 100 MHz): δ 170.31, 154.73, 153.72, 150.66, 140.71, 137.46, 136.91, 130.67, 128.06, 126.59, 126.18, 124.09, 122.38, 121.57, 119.10, 113.51, 78.93, 76.49, 58.22 **ESI-MS**: calcd. for C₁₉H₁₂N₂OSH⁺[M+H]⁺ 316.0670, found 317.0748

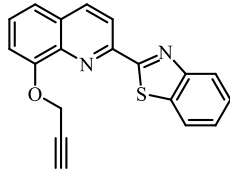
8.298
8.277
8.142
8.122
7.996
7.976
7.553
7.543
7.540
7.532
7.530
7.525
7.520
7.509
7.505
7.502
7.461
7.458
7.440
7.423
7.420
7.361
7.350
7.339
7.328
7.317
5.163
5.157
2.586
2.580
2.574



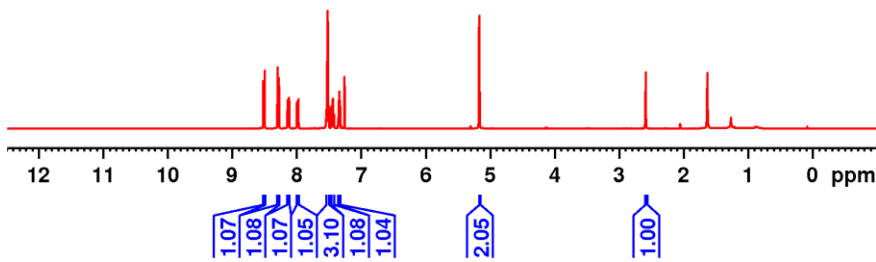
Current Data Parameters
NAME SRK-AS-03-1H
EXPNO 10
PROCNO 1

F2 - Acquisition Parameters
Date_ 20230413
Time 19.20 h
INSTRUM Avance Neo 400
PROBHD Z163739_0226 ()
PULPROG zg30
TD 51724
SOLVENT CDC13
NS 18
DS 0
SWH 8620.689 Hz
FIDRES 0.333334 Hz
AQ 2.9999919 sec
RG 101
DW 58.000 usec
DE 13.14 usec
TE 297.7 K
D1 1.00000000 sec
TD0 1
SFO1 400.1324708 MHz
NUC1 1H
P0 2.67 usec
P1 8.00 usec
PLW1 25.07999992 W

F2 - Processing parameters
SI 65536
SF 400.1300100 MHz
WDW EM
SSB 0
LB 0.30 Hz
GB 0
PC 1.00



(a)



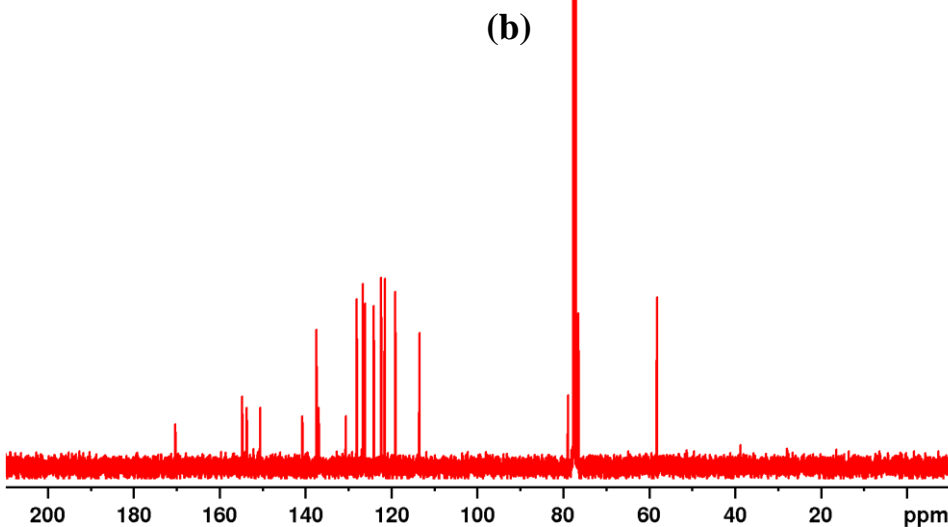
170.31
154.74
153.73
150.60
140.72
137.46
136.91
130.67
128.06
126.60
126.19
124.10
122.39
121.58
119.11
113.51
78.94
76.50
58.23



Current Data Parameters
NAME SRK-AS-03-13C
EXPNO 12
PROCNO 1

F2 - Acquisition Parameters
Date_ 20230413
Time 19.27 h
INSTRUM Avance Neo 400
PROBHD Z163739_0226 ()
PULPROG zgpg30
TD 65536
SOLVENT CDC13
NS 200
DS 0
SWH 27777.777 Hz
FIDRES 0.847710 Hz
AQ 1.1796480 sec
RG 101
DW 18.000 usec
DE 6.50 usec
TE 298.3 K
D1 1.00000000 sec
D11 0.03000000 sec
TD0 1
SFO1 100.6242384 MHz
NUC1 13C
P0 2.67 usec
P1 8.00 usec
PLM1 99.3399634 W
SFO2 400.1316005 MHz
NUC2 1H
CPDPRG2 waltz65
PCPD2 90.00 usec
PLW2 25.07999992 W
PLW12 0.19815999 W
PLW13 0.09967500 W

F2 - Processing parameters
SI 32768
SF 100.6127356 MHz
WDW EM
SSB 0
LB 1.00 Hz
GB 0
PC 1.40



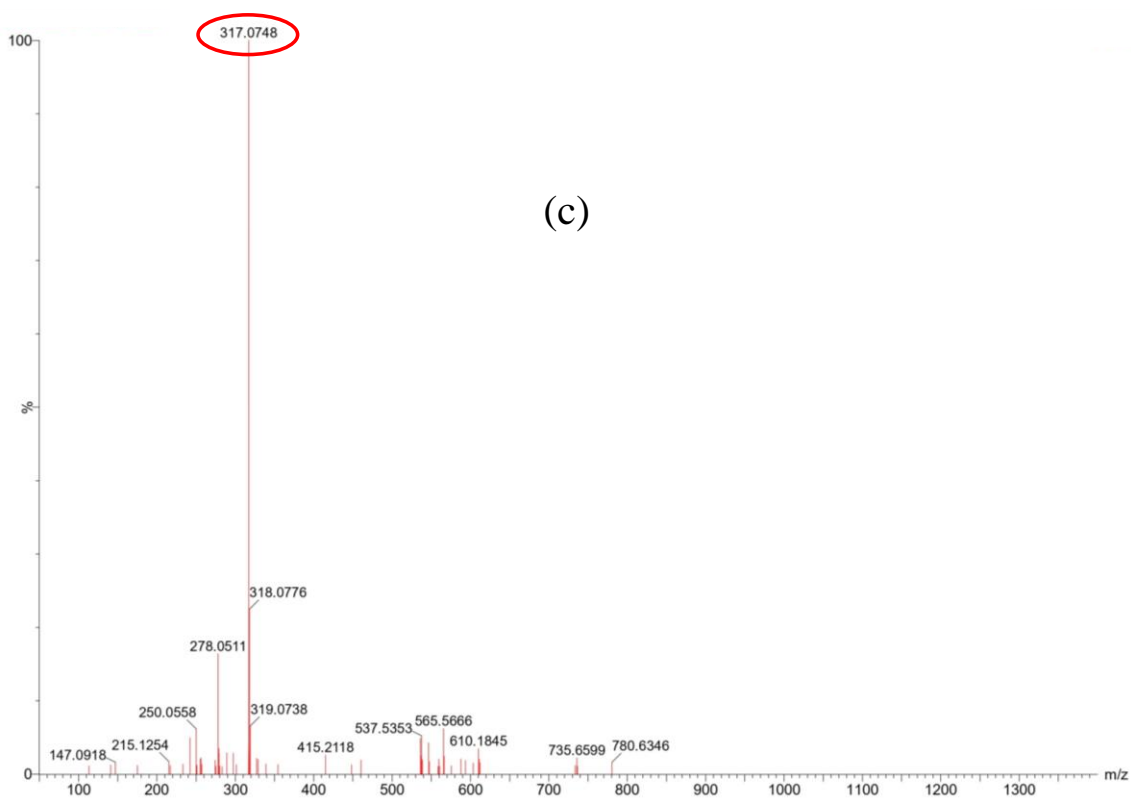


Fig. S2. (a) ^1H NMR (CDCl_3), (b) ^{13}C NMR (CDCl_3) and (c) ESI-MS spectrum of compound **P₃**

S3. Synthesis and Characterization of Compound **P₅**

The **P₅** has been synthesized by a producer in the reported literature². The final yield was 61% resulting in off-white crystal. **^1H NMR (CDCl_3 , 600 MHz):** δ 5.15 (t, $J=9.50$ Hz, 1 H), 5.04 (t, $J=9.70$ Hz, 1H), 4.89 (t, $J=9.20$ Hz, 1H), 4.60 (d, $J=8.90$ Hz, 1H), 4.21 (dd, $J=12.40$ Hz, $J=4.45$ Hz, 1H), 4.10 (d, $J=12.40$ Hz, 1H), 3.74 (dd, $J=9.96$ Hz, 1H), 2.03 (s, 3H), 2.01 (s, 3H), 1.96 (s, 3H), 1.94 (s, 3H) **^{13}C NMR (CDCl_3 , 150 MHz):** δ 170.82, 170.33, 169.54, 169.43, 88.11, 74.24, 72.82, 70.86, 68.12, 61.89, 20.92, 20.78, 20.76

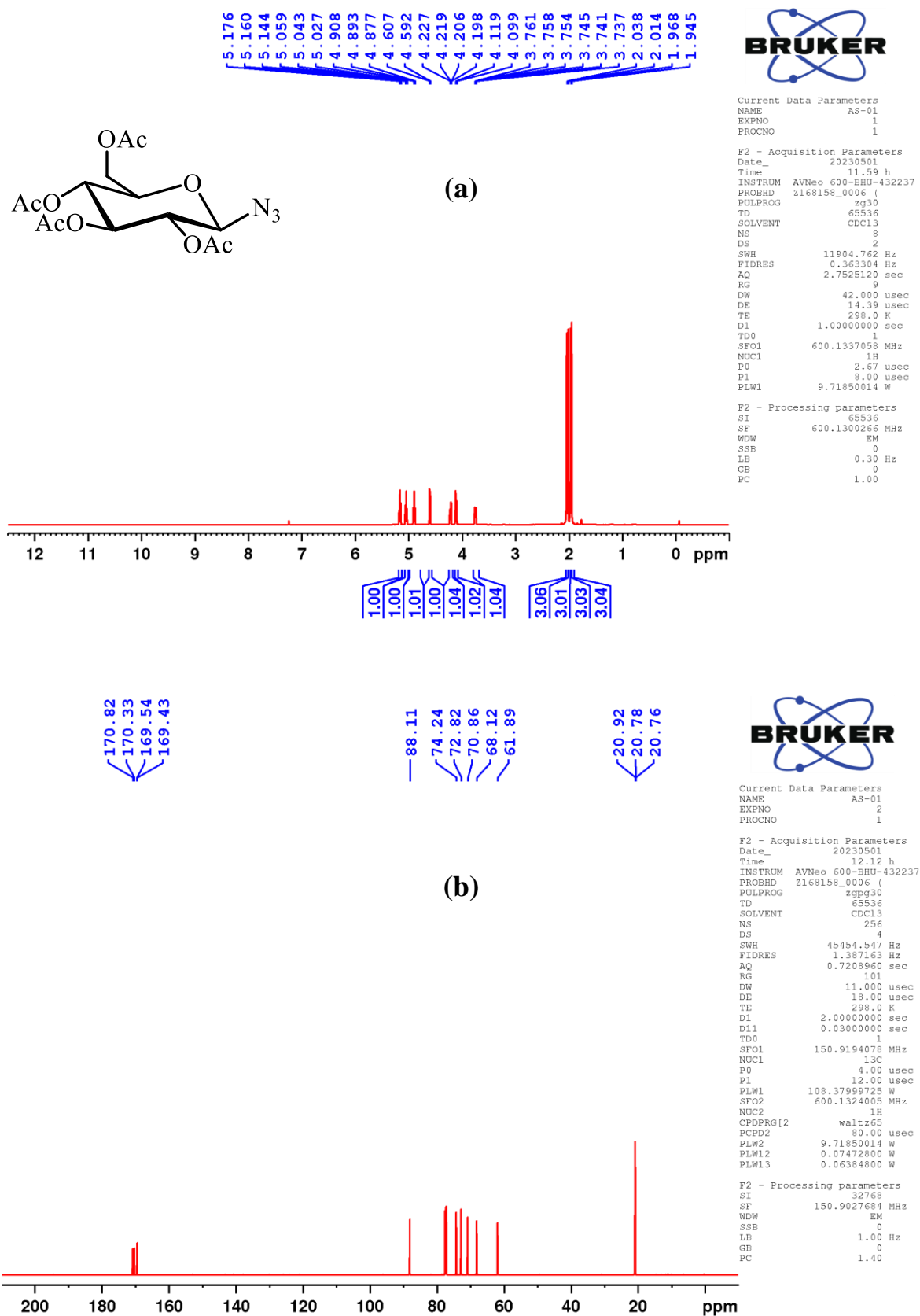
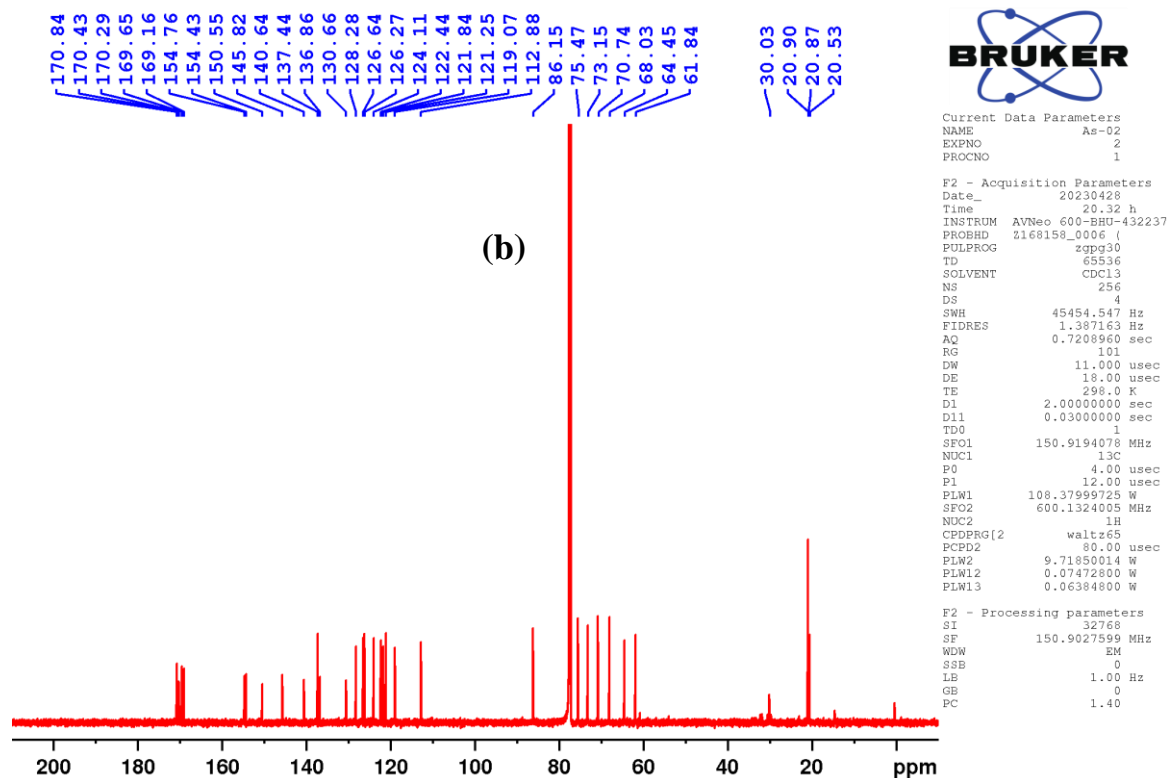
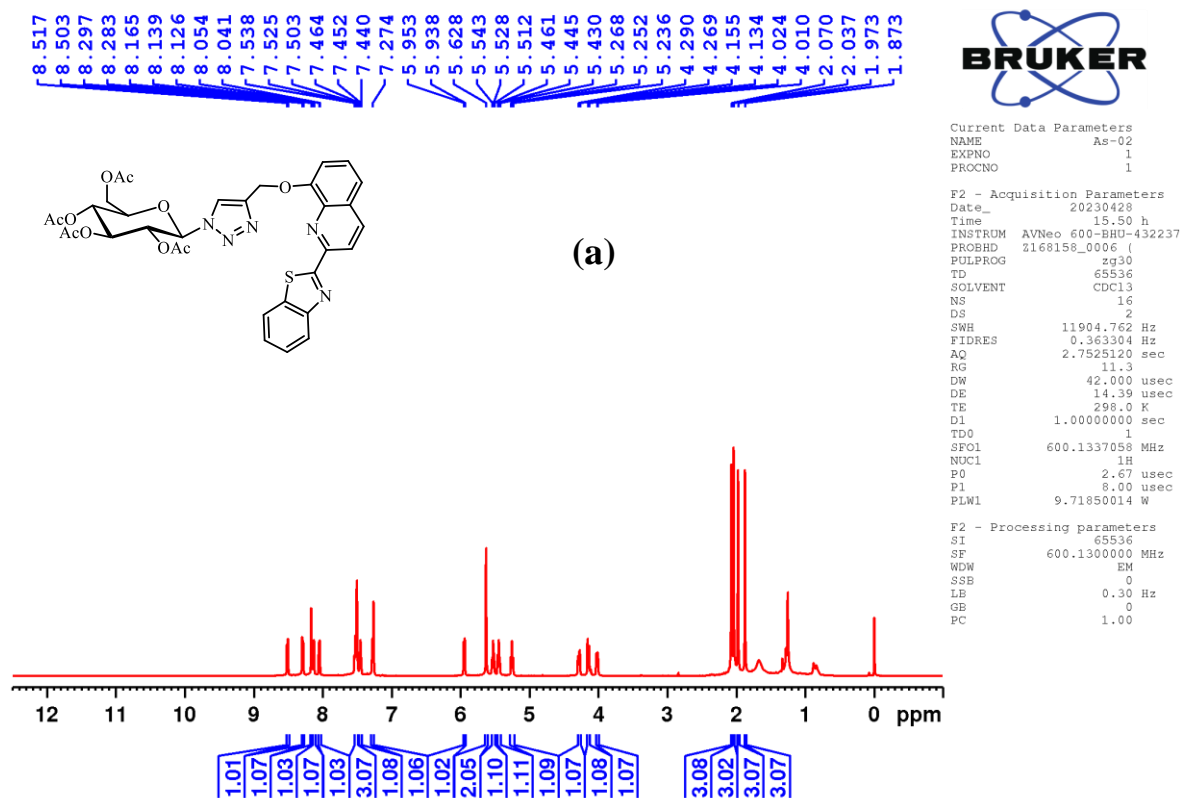


Fig. S3. Spectrum of compound **P5** in CDCl_3 (a) ^1H NMR and (b) ^{13}C NMR

S4. Characterization of compound P₆



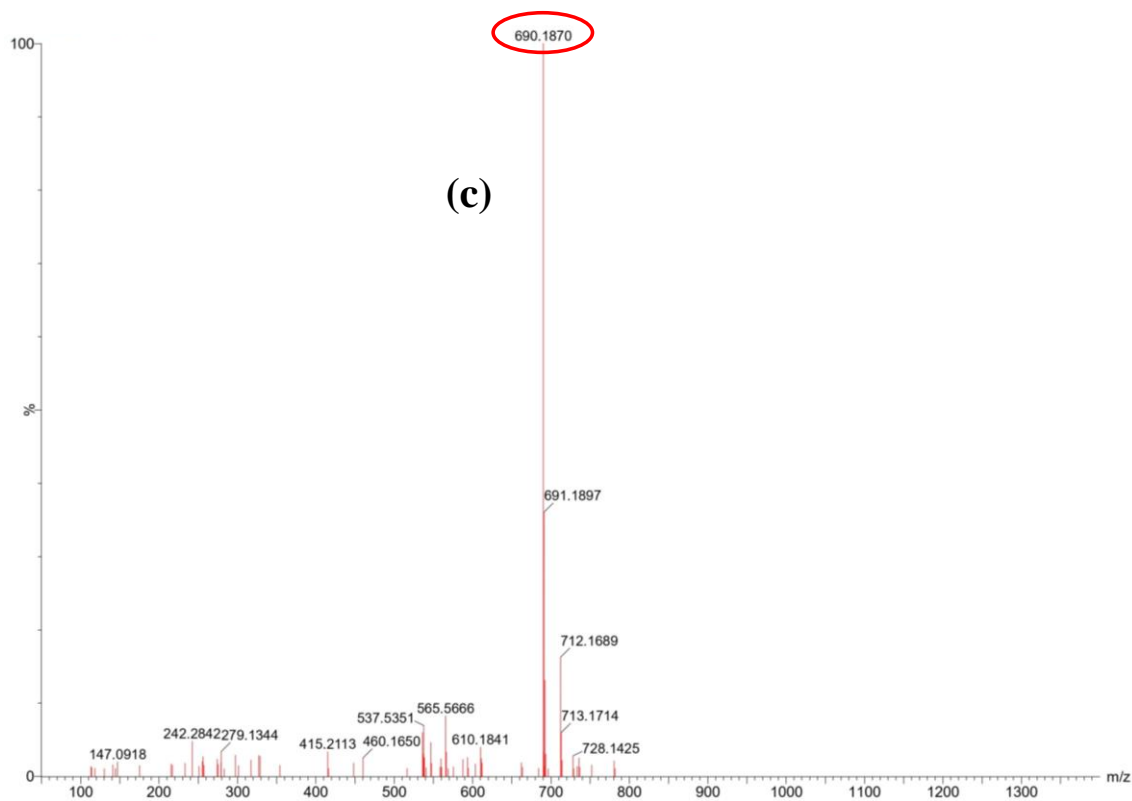
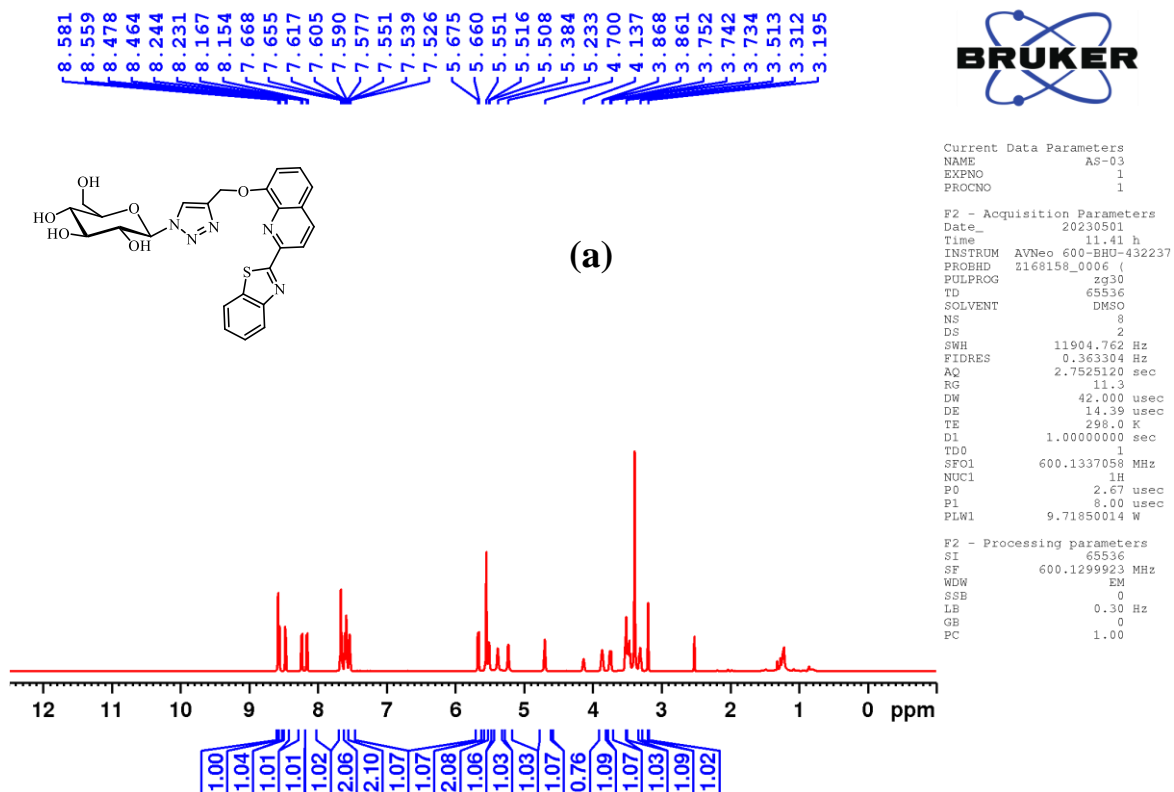


Fig. S4: (a) ^1H NMR (CDCl_3), (b) ^{13}C NMR (CDCl_3) and (c) ESI-MS spectrum of compound **P6**

S5. Characterization of compound **L**



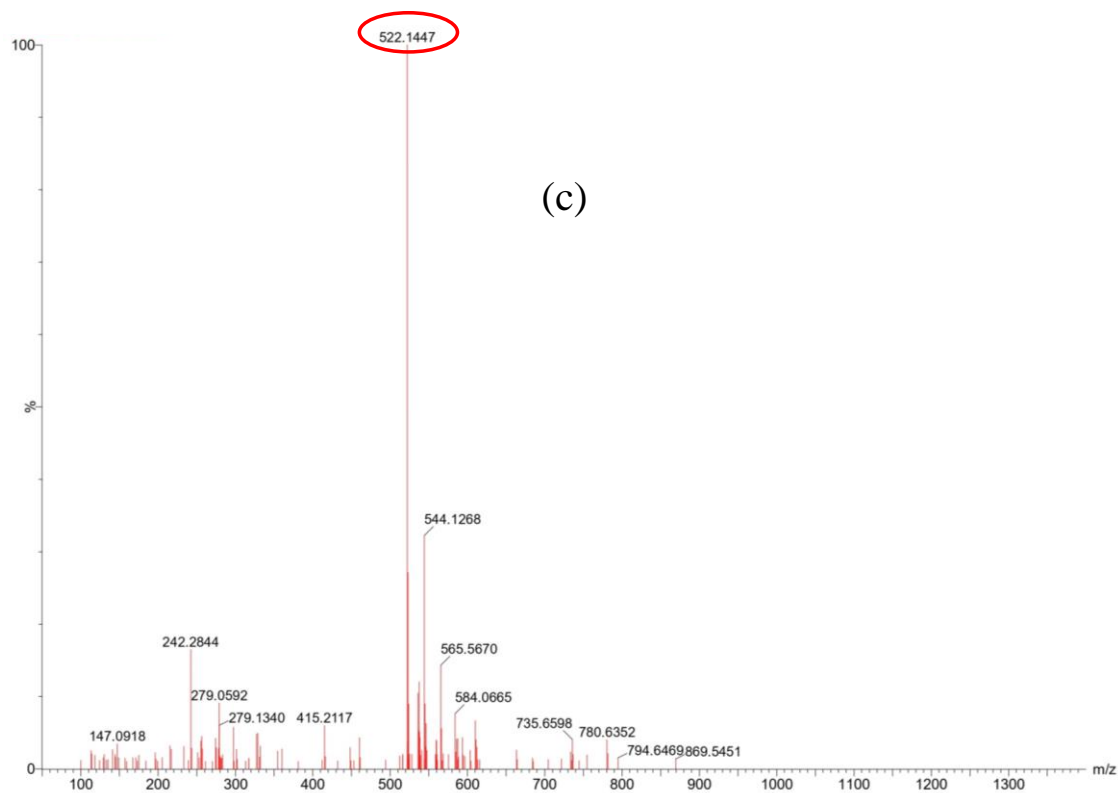
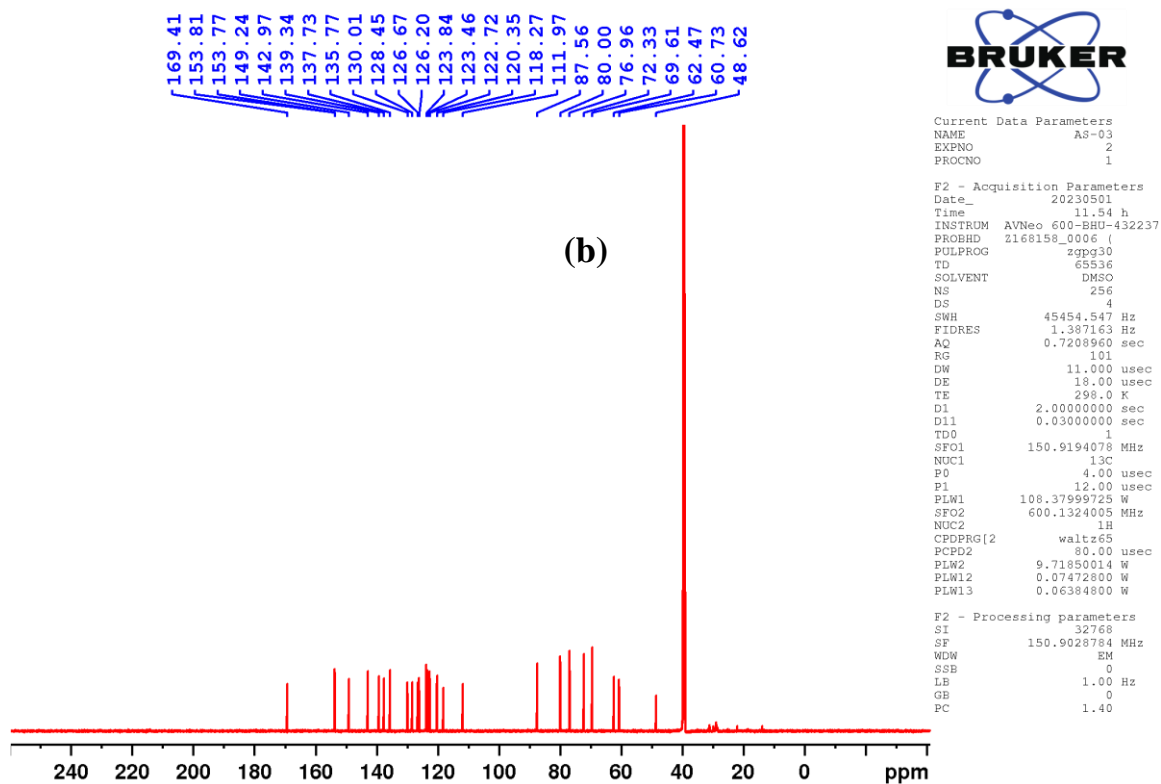


Fig. S5. (a) ^1H NMR (DMSO- d_6), (b) ^{13}C NMR (DMS)- d_6 and (c) ESI-MS spectrum of compound **L**

S6. Solubility of probe L in water

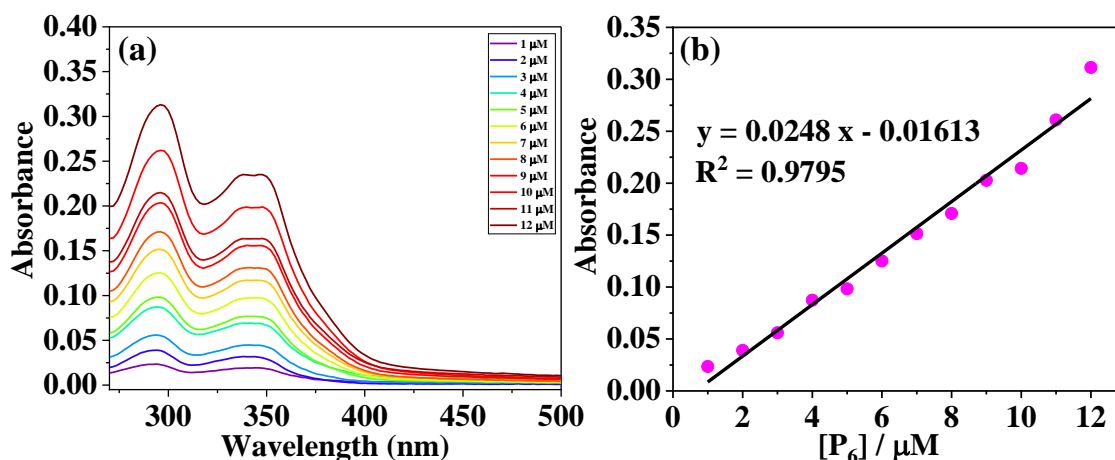


Fig. S6 (a) UV-Vis spectra of **L** at different concentrations ranging from 1-12 μM in water (b) A plot of absorbance (294 nm) vs. different concentrations of **L** in water.

S7. Effect of absorbance and Fluorescence on probe L using different metal ions

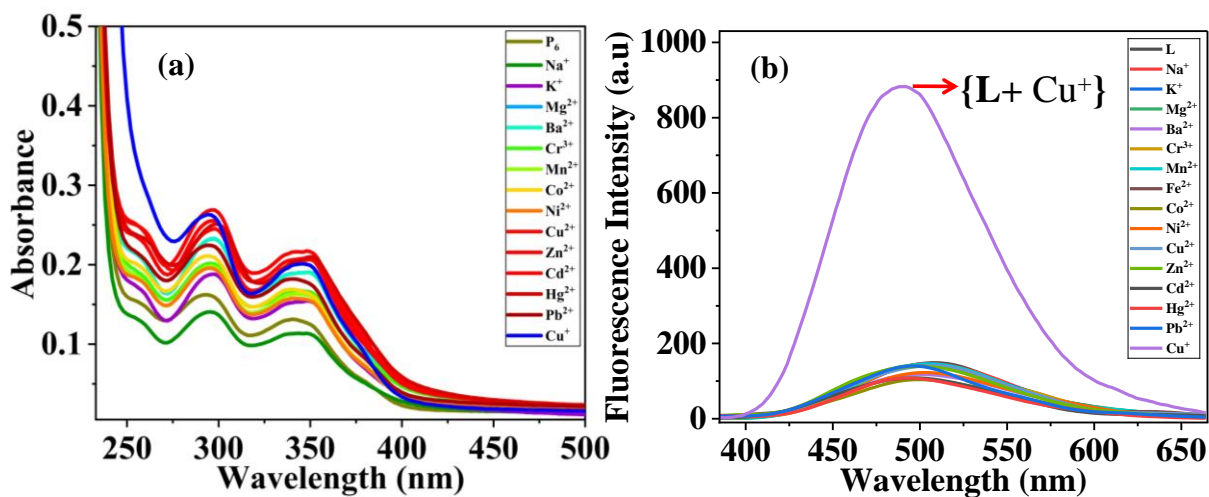


Fig. S7 (a) Absorbance of **L** (10 μM) with Cu^+ (3 equivalent) and other metal ions (10 equivalent) in water (b) fluorescence spectral titration of **L** (10 μM) with Cu^+ (3 equivalents) and other different metals (10 equivalents) ($\lambda_{\text{ex}}=294$ nm) in water.

S8 Fluorescence spectra of L with different metal ions

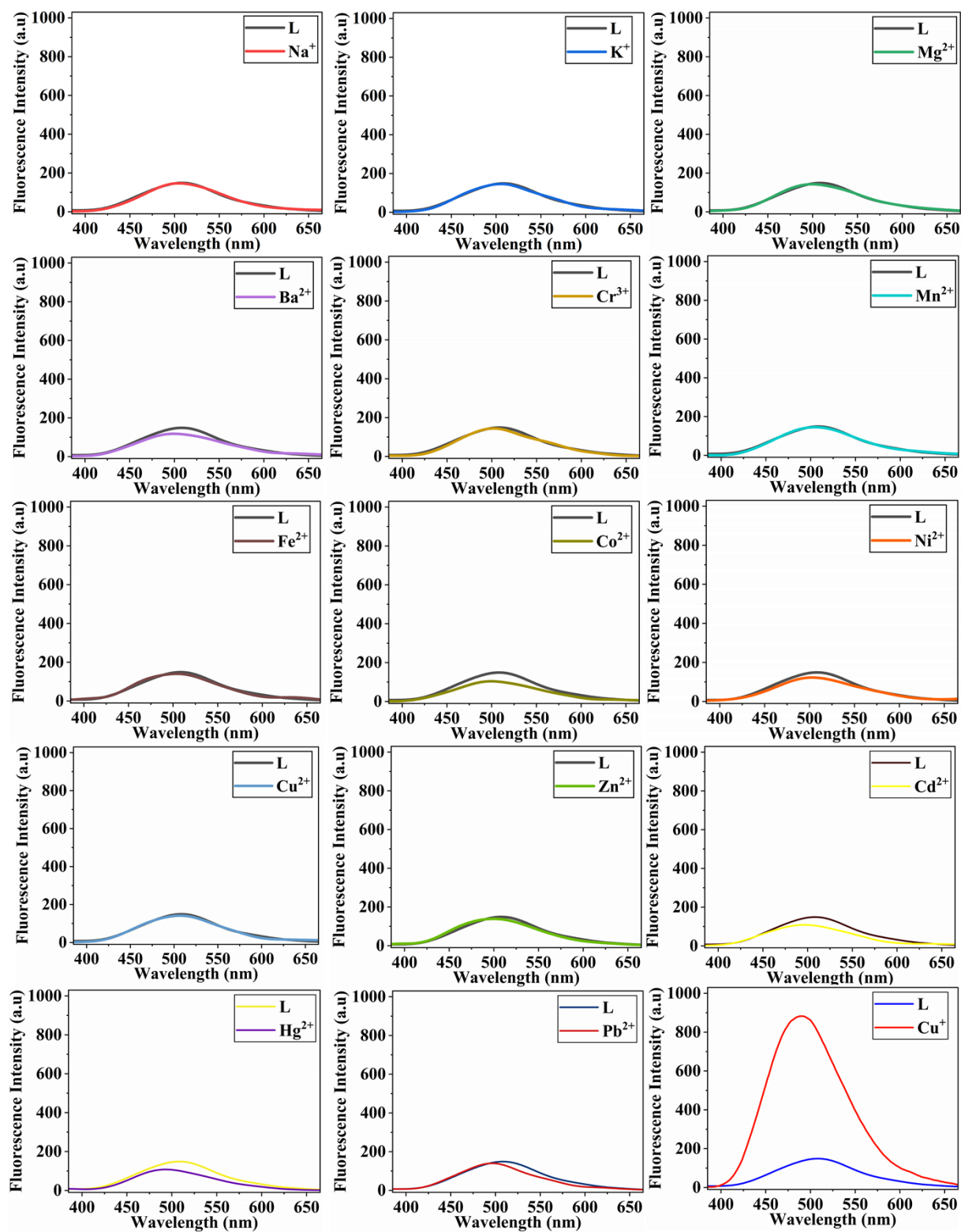


Fig. S8. Fluorescence spectra of L (10 μ M) titrated with various metal ions (10 equivalents) in water.

S9. Association constant obtained from the fluorescence titration of {L+Cu⁺} complex

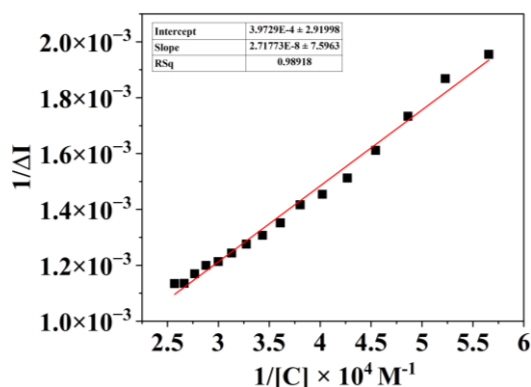


Fig. S9. Binding constant (K_a) of Ligand **L** with Cu^+ concentration in water

S10. Determination of Limit of Detection (LOD) of Cu^+ by **L**

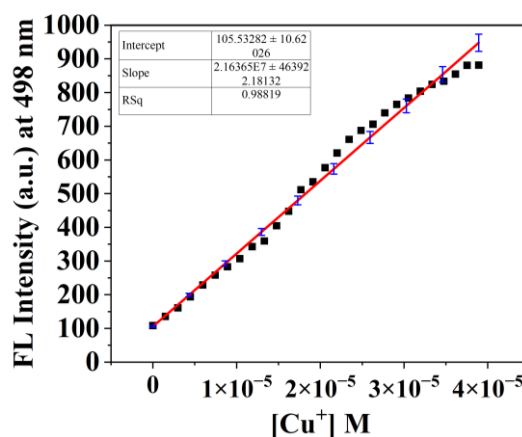


Fig. S 10. Linear fluorescence relationship of Ligand (**L**) with Cu^+ (3-90 μM) in water at $\lambda_{\text{em}}=498 \text{ nm}$

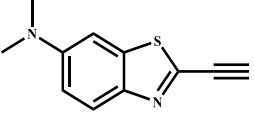
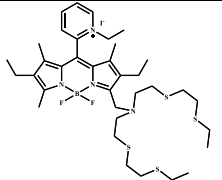
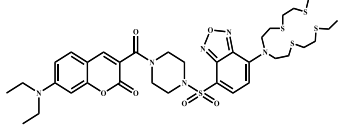
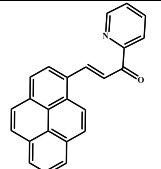
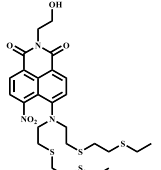
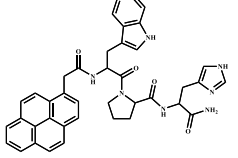
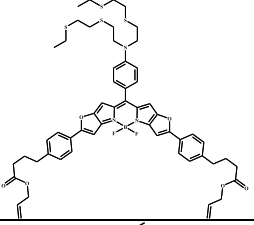
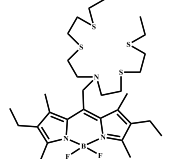
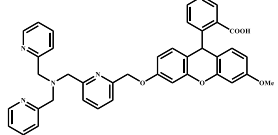
S11. Fluorescence quantum yield of **L** and {L+ Cu^+ } complex

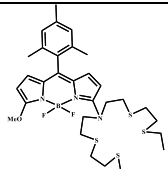
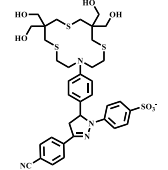
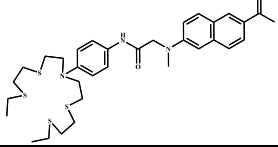
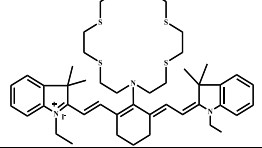
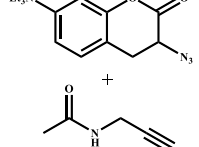
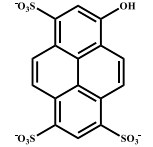
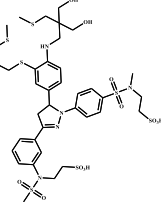
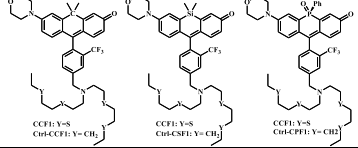
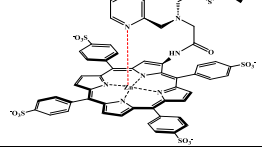
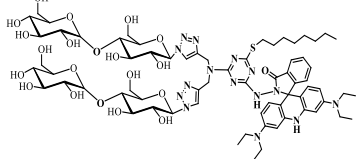
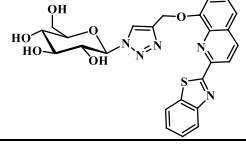
The quantum yield (Φ) was determined using literature reported method by the following equation.³

$$\Phi Y_{\text{sample}} = \Phi Y_{\text{Reference}} \left(\frac{\text{sample gradient}}{\text{reference gradient}} \right) \left(\frac{\text{sample refractive index}}{\text{reference refractive index}} \right)^2$$

where the subscripts R and S denote the reference standard (fluorescein in 0.1 M NaOH) and the synthesized sample **L**, respectively. Φ represents the quantum yield, F is the integrated fluorescence emission, A is the absorbance at the excitation wavelength, and n is the refractive index of the solvent. The quantum yield of **L** was calculated using fluorescein as the standard, which has a reported quantum yield of 0.79 in 0.1 M NaOH.

S12. Table 1: Comparisons between **L** and the molecular probes reported in the literature.

Sr. No.	Fluorescent molecular systems	Ion	Limit of detection (LOD)	Solvent system	Ref.
1.		Cu ⁺	N.R	PBS buffer (1 mM, pH 7.2)	[31] <i>Bioorg. Med. Chem. Lett.</i> , 2012, 22 , 1747–1749.
2.		Cu ⁺	N.R	HEPES buffer (10 mM, pH 7.2)	[32] <i>Chem. Commun.</i> , 2014, 50 , 9835–9838.
3.		Cu ⁺	N.R	Tris-HCl buffer/DMF 4:6 v/v pH=7.2	[33] <i>Sci. China: Chem.</i> , 2019, 62 , 465–474.
4.		Cu ⁺	1.2 × 10 ⁻⁹ M	SDS (8 mM) micelles (EDTA 2 μM)	[34] <i>J. Mater. Chem. B</i> , 2023, 11 , 4111-4120
5.		Cu ⁺	N.R	HEPES buffer solution (with 50% of acetonitrile, pH 7.2)	[35] <i>Chem. Commun.</i> , 2013, 49 , 5565–5567.
6.		Cu ⁺	N.R	(10 mM HEPES, pH 7.4) containing 1% DMF	[36] <i>Sensors and Actuators B</i> , 2018, 256 , 393–401.
7.		Cu ⁺	N.R	Thiourea buffer in methanol	[37] <i>Angew. Chem., Int. Ed.</i> , 2021, 133 , 23332–23337.
8.		Cu ⁺	N.R*	HEPES buffer (20 mM, pH 7)	[38] <i>J. Am. Chem. Soc.</i> 2006, 128 , 10–11
9.		Cu ⁺	N.R	HEPES buffer (50 mM, pH 7.2)	[39] <i>J. Am. Chem. Soc.</i> 2010, 132 , 5938–5939

10.		Cu ⁺	N.R	HEPES buffer (20 mM, pH 7.0)	[40] <i>J. Am. Chem. Soc.</i> , 2010, 132 , 1194–1195.
11.		Cu ⁺	N.R	MOPS/K ⁺ , (10 mM, pH 7.2)	[41] <i>J. Am. Chem. Soc.</i> 2011, 133 , 15906–15909
12.		Cu ⁺	N.R	HEPES buffer (20 mM, pH 7.0)	[42] <i>Chem. Commun.</i> , 2011, 47 , 7146–7148.
13.		Cu ⁺	4.1×10^{-13} M	PBS Buffer (25 mM, pH 7.0)	[43] <i>Chem. Commun.</i> , 2012, 48 , 6247–6249.
14.		Cu ⁺	2.0×10^{-7} M	HEPES Buffer (0.10 M, pH 7.4)	[44] <i>Tetrahedron Lett.</i> , 2012, 53 , 4473–4475.
15.		Cu ⁺	1.0×10^{-6} M	Water	[45] <i>Photochem. Photobiol. Sci.</i> , 2014, 13 , 1427–1433.
16.		Cu ⁺	7.5×10^{-12} M	pH 6 buffer (10 mM MES, 100 nM MCL-1)	[46] <i>Chem. Sci.</i> , 2016, 7 , 1468–1473
17.		Cu ⁺	N.R	Thiourea-buffered	[47] <i>ACS Chem. Biol.</i> 2018, 13 , 1844–1852
18.		Cu ⁺	8.2×10^{-9} M	PBS (20 mM, pH 7.0)	[48] <i>ACS Sens.</i> , 2019, 4 , 856–864.
19.		Cu ⁺	2.0×10^{-8} M	PBS Buffer (10 mM, pH 7.0)	[49] <i>ACS Sens.</i> 2024, 9 , 1419–1427
20.		Cu ⁺	1.48×10^{-8} M	Water	Present work

*N.R. represents LOD not reported

S13. Reversibility experiments of L with Cu⁺

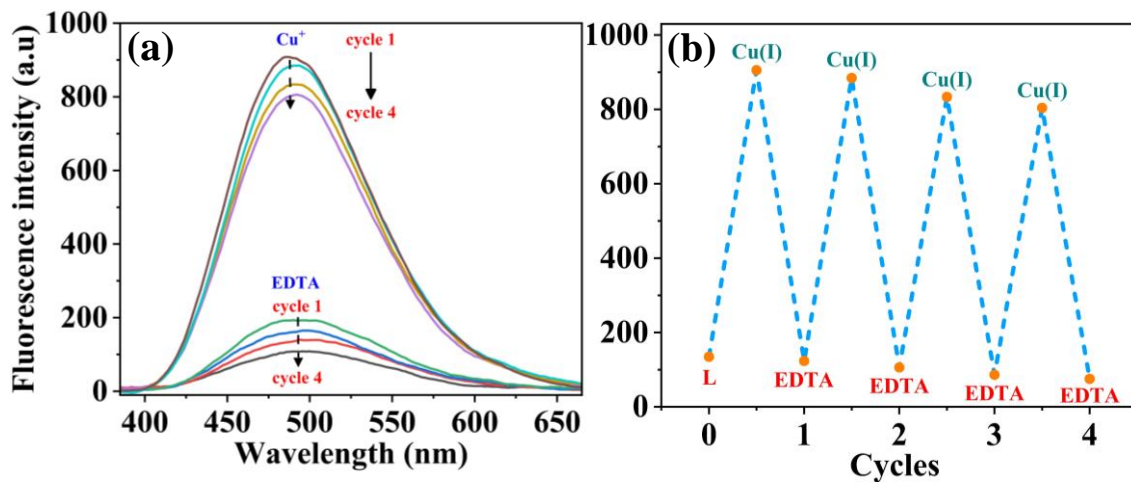


Fig. S13. (a) Fluorescence switching plot of **L** ($n=4$) after repeated additions of Cu^+ followed by EDTA showing the reversibility of **L** (b) Reversible fluorescence up to four cycles of **L** with Cu^+ ($n=4$).

S14. Optimized structure of L and {L+Cu⁺}

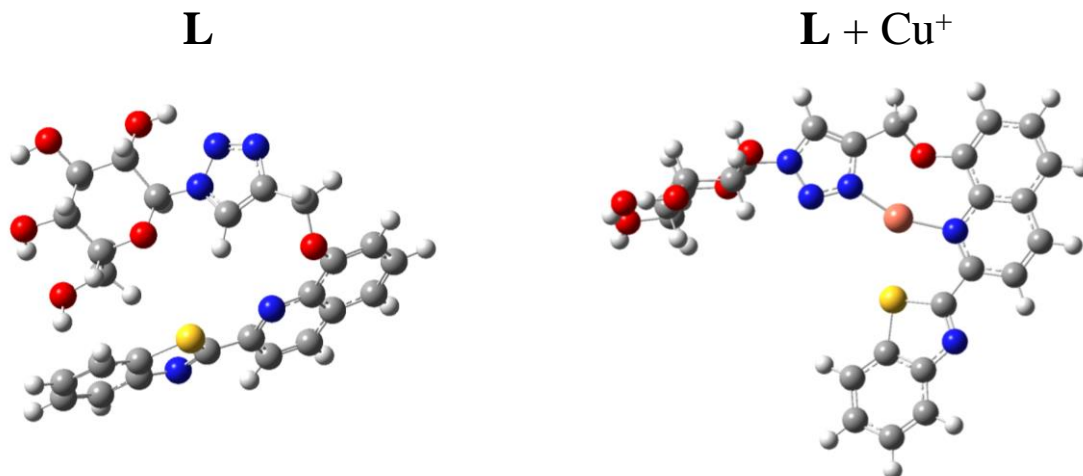


Fig. S14. Theoretical optimized structure of **L** and $\{\text{L}+\text{Cu}^+\}$

Table S 01. Cartesian coordinates of optimized L

Z	Coordinates			Z	Coordinates		
	X	Y	X		X	Y	Z
6	-1.98537	3.353833	-0.261477	1	3.372344	2.236552	2.968243
6	-1.00661	2.171346	-0.364928	8	3.73345	0.667185	1.76665
6	-2.70633	0.505563	-0.077015	6	4.331172	0.235729	0.620983
6	-3.75362	1.609585	0.079694	6	3.671765	-0.782799	-0.135165
6	-3.36584	2.875512	-0.684708	6	5.552688	0.706802	0.208751
1	-0.83092	1.969984	-1.430591	6	4.298129	-1.272246	-1.314017
1	-2.03484	3.675495	0.788766	6	6.164744	0.20606	-0.959069
1	-2.91865	-0.2876	0.646316	1	6.056358	1.465518	0.797125
1	-3.79111	1.881099	1.141289	6	1.836555	-2.121246	-0.462175
1	-3.32876	2.661	-1.765652	6	3.597205	-2.249605	-2.06335
8	-1.43384	1.015054	0.313662	6	5.557025	-0.764079	-1.708778
8	-1.58106	4.387103	-1.116895	1	7.130978	0.599474	-1.256147
1	-0.71984	4.695838	-0.789909	6	2.366046	-2.671617	-1.655199
8	-4.30977	3.881532	-0.418257	1	4.049353	-2.645151	-2.967818
1	-5.17187	3.449971	-0.508742	1	6.023559	-1.148198	-2.609986
8	-5.05787	1.203634	-0.284537	1	1.784782	-3.400822	-2.205018
1	-4.9773	0.53444	-0.985887	7	2.459984	-1.23089	0.274103
6	-2.65533	-0.143205	-1.465555	6	-1.5634	-2.823092	1.264316
1	-2.5479	0.598873	-2.259758	6	-1.5666	-3.284189	-0.066098
1	-1.79277	-0.816466	-1.516747	6	-2.73043	-3.841811	-0.609199
8	-3.87109	-0.829472	-1.740666	6	-3.86153	-3.930207	0.184654
1	-3.88814	-1.640065	-1.210982	6	-3.84564	-3.475188	1.512856
7	0.280002	2.490575	0.249584	6	-2.70229	-2.922509	2.064536
6	1.13087	1.650662	0.87155	6	0.494617	-2.516951	-0.003332
6	2.213338	2.439866	1.171478	1	-2.72142	-4.196327	-1.633951
1	0.926045	0.608197	1.037411	1	-4.7693	-4.366286	-0.218778
7	0.802078	3.724581	0.164501	1	-4.74296	-3.557646	2.11633
7	1.973661	3.697162	0.723331	1	-2.69655	-2.569294	3.089759
6	3.467963	2.062741	1.893646	7	-0.38025	-3.102033	-0.752359
1	4.298713	2.67443	1.529172	16	-0.00823	-2.137049	1.638587

Table S 02. Cartesian coordinates of optimized {L+Cu⁺}

Z	Coordinates			Z	Coordinates		
	X	Y	X		X	Y	Z
6	5.562101	-0.02528	-1.00067	1	-2.9532	-5.07694	-0.76039
6	5.995367	0.53164	0.361971	6	-1.90957	3.72889	-0.27104
6	5.645415	-0.46792	1.450803	6	-3.14142	3.971464	0.36523
1	6.189418	-0.89828	-1.23314	6	-3.48848	5.273292	0.740823
1	6.237744	-1.37967	1.268324	6	-2.60227	6.296967	0.471793
1	5.445535	1.467594	0.551425	6	-1.37781	6.042246	-0.16445

8	4.181188	-0.40246	-0.97981	6	-1.0156	4.760623	-0.54255
7	2.448804	-1.65578	-0.1371	6	-3.34578	1.791197	0.1287
6	1.884187	-2.86218	-0.37644	1	-4.43817	5.450675	1.231709
6	0.538986	-2.62192	-0.35295	1	-2.85293	7.313189	0.754403
1	2.466057	-3.75625	-0.53041	1	-0.70085	6.865542	-0.36456
7	1.541046	-0.71116	0.025751	1	-0.06841	4.570474	-1.03385
7	0.381121	-1.28938	-0.10299	16	-1.76652	2.024776	-0.62308
6	-0.65361	-3.52194	-0.48799	7	-3.9263	2.85369	0.567433
1	-0.46561	-4.31152	-1.22116	6	5.668794	0.995651	-2.12208
1	-0.89935	-3.98918	0.472147	1	5.39336	0.52339	-3.07235
8	-1.73786	-2.69349	-0.90615	1	4.95608	1.806235	-1.9206
6	-3.01218	-2.96696	-0.48057	8	7.006563	1.464782	-2.13758
6	-3.79576	-1.83664	-0.11099	1	7.104668	2.141468	-2.8162
6	-5.15417	-2.03193	0.224956	8	7.385465	0.718394	0.446237
6	-4.89965	-4.41089	-0.08417	1	7.654589	1.248697	-0.32041
6	-3.9713	0.464808	0.183237	8	5.895575	0.031964	2.741255
6	-5.91662	-0.88036	0.544079	1	6.818478	0.320539	2.761981
6	-5.68977	-3.34104	0.238288	8	3.857349	-1.85995	2.304259
1	-5.30859	-5.41459	-0.07403	1	4.268287	-1.62269	3.147748
6	-5.34208	0.356025	0.506192	6	3.869172	-1.34436	0.000353
1	-6.96362	-0.99516	0.80551	1	4.397133	-2.29517	-0.15749
1	-6.73117	-3.4801	0.506806	6	4.174901	-0.83197	1.401562
1	-5.8892	1.263882	0.723357	1	3.572544	0.069076	1.580997
7	-3.21576	-0.59286	-0.08251	29	-1.34828	-0.60671	-0.17057
6	-3.55239	-4.22419	-0.46138				

S15. Effect of pH on the fluorescence emission of L and {L+Cu⁺}

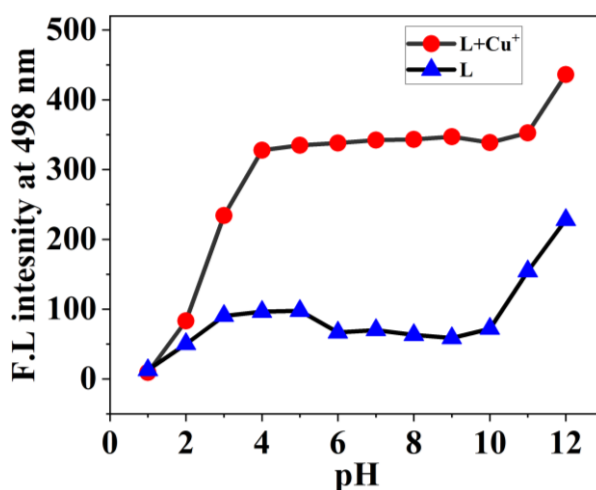


Fig. S15. Fluorescence response of (a) Free L (10 μ M), (b) in the presence of Cu⁺ (1 equiv.), and (c) fluorescence emission at 498 vs. pH range from 1-12.

References:

- 1 S. Areti, S. Bandaru, R. Teotia and C. P. Rao, Water-Soluble 8-Hydroxyquinoline Conjugate of Amino-Glucose As Receptor for La^{3+} in HEPES Buffer, on Whatman Cellulose Paper and in Living Cells, *Anal. Chem.*, 2015, **87**, 12348–12354.
- 2 N. Drillaud, E. Banaszak-Leonard, I. Pezron and C. Len, Synthesis and Evaluation of a Photochromic Surfactant for Organic Reactions in Aqueous Media, *J. Org. Chem.*, 2012, **77**, 9553–9561.
3. J. Hu and C.-y. Zhang, Quantum Yield Limits for the Detection of Single-Molecule Fluorescence Enhancement by a Gold Nanorod, *Anal. Chem.*, 2013, **85**, 2000–2004.